Norwegian University of Life Sciences
Faculty of Environmental Sciences and
Natural Resource Management

Philosophiae Doctor (PhD)
Thesis 2017:69

Biomass stock and change estimation in boreal forests using remotely sensed data – results from empirical studies and simulations

Estimering av biomasse og biomasse-endringer i
boreal skog ved bruk av fjernmålte
data – resultater fra empiriske studier og simuleringer

Victor Felix Strîmbu

Biomass stock and change estimation in boreal forests using remotely sensed data – results from empirical studies and simulations

Estimering av biomasse og biomasse-endringer i boreal skog ved bruk av fjernmålte data – resultater fra empiriske studier og simuleringer

Philosophiae Doctor (PhD) Thesis

Victor Felix Strîmbu

Faculty of Environmental Sciences and Natural Resource Management
Norwegian University of Life Sciences

Ås 2017

Thesis number 2017:69
ISSN 1894-6402
ISBN 978-82-575-1465-5

PhD supervisors

Professor Erik Næsset
Faculty of Environmental Sciences and Natural Resource Management
Norwegian University of Life Sciences
Postbox 5003, 1432 Ås, Norway

Dr. Liviu T. Ene
Faculty of Environmental Sciences and Natural Resource Management
Norwegian University of Life Sciences
Postbox 5003, 1432 Ås, Norway

Dr. Rasmus Astrup
Norwegian Institute of Bioeconomy Research
Postbox 115, 1431 Ås, Norway

Evaluation committee

Professor Ross Nelson
Biospheric Sciences Lab, Code 618
NASA – Goddard Space Flight Center
20771 Greenbelt, Maryland, USA

Professor Göran Ståhl
Department of forest Resource Management
Swedish University of Agricultural Sciences
90183 Umeå, Sweden

Dr. Ole Martin Bollandsås
Faculty of Environmental Sciences and Natural Resource Management
Norwegian University of Life Sciences
Postbox 5003, 1432 Ås, Norway

Acknowledgements

This PhD was a unique experience for which I am thankful. I was given the opportunity to expand my knowledge and make a small contribution. It is a pleasure to thank those who made this possible.

First, I would like to gratefully acknowledge my advisors Prof. Erik Næsset, Dr. Liviu Ene, and Dr. Rasmus Astrup. Liviu has been a great mentor whom I owe a great deal of everything I learned. Special thanks goes to Prof. Terje Gobakken for offering his help whenever needed.

My gratitude extends to Prof. Timothy Gregoire, who generously hosted me at Yale School of Forestry & Environmental Studies in 2016. It was a memorable experience, and a chance to make new friends. Cheers to Peter, Dea, Rita, Kezang, Sonam and Henry! Likewise, I would like to thank Prof. Ronald McRoberts for having me at the US Forest Services, in St. Paul, Minnesota.

I thank my colleagues in the skogrover group: Ole Martin, Hans Ole, Marius, Daud, Stefano, Endre, and Ernest. Stefano, you were a great office mate. Thank you for all the stimulating discussions! My warmest thanks to all the friends that I made here, Kaja, Patricia, Marek, Agnieszka, Rafał, Carolina, Stefano, Walid, many others, and to a very special girl, Sara.

Finally, I would like to thank my family, my parents and brother, for all the moral support, and uncle Bogdan whose influence was decisive when I started on this path.

Victor Strîmbu

Ås, 9. July, 2017

Contents

List of papers

Paper I: Strîmbu, V.F., Ene, Liviu T., Næsset, E. (2016). Spatially consistent imputations of forest data under a semivariogram model. *Canadian Journal of Forest Research*, 46, 1145-1156.

Paper II: Strîmbu, V.F., Ene, Liviu T., Gobakken, T., Gregoire, T.G., Astrup, R., Næsset, E. (2017). Post-stratified change estimation for large-area forest biomass using repeated ALS strip sampling. *Canadian Journal of Forest Research*, 47, 839-847.

Paper III: Strîmbu, V.F., Ene, Liviu T., Gobakken, T., Næsset, E. (manuscript). Simulative assessment of model assisted and hybrid estimation of change using repeated ALS sampling.

Abstract

Airborne LiDAR (Light Detection and Ranging) has become an important remote sensing tool for forest inventory. In the past two decades, this technology has seen a rapid status transition from experimental to operational, mainly driven by the cost saving – precision increasing duality and paralleled by accelerating technological availability. For large-area resource estimation, airborne laser scanning (ALS) has been proposed as a sampling tool. Two-stage model assisted (MA) and two-phase hybrid (HY) estimators have been proposed for this type of survey. This thesis investigated biomass stocks and biomass change estimation using repeated ALS strip sampling survey and national forest inventory field data. Emphasis was on simulative methods to assess the properties of the estimators.

Initially, a method to perform spatially consistent nearest neighbor imputations of forest data was developed (*paper I*). The method was used to generate spatially explicit forest populations with realistic spatial structure under a prescribed semivariogram model. In addition, the population distribution was controlled by a prescribed histogram. The method was tested in a small forest area (Våler municipality, Norway) using wall-to-wall ALS data, Landsat 7 imagery, and a dense network of field plots that facilitated semivariogram analysis.

In *paper II*, MA and HY post-stratified estimators were used to estimate above ground biomass (AGB) stock and change over a period of five years in the southern portion of Hedmark County, Norway. The reference points in time were 2006 and 2011. A nested post-stratification scheme was trialed, combining land cover classes with change classes. Parametric bootstrapping was demonstrated as a simulative alternative to estimate the model uncertainty component in the hybrid estimator.

Finally, in *paper III* a practical methodology to create realistic artificial forest populations for two points in time was proposed, using multiple sources of empirical data and prescribed parameters. To this end, the method of *paper I* was combined with a copula approach to model multivariate relationships, preserving the integrity of the multivariate relationship both horizontally (ALS-AGB) and longitudinally between the two points in time. The method ensured that different types of change were proportionally represented in the artificial population. Sampling simulations were performed on a surrogate population tailored to the southern portion of Hedmark County. The simulations closely followed the actual Hedmark survey rather than the theoretical multi-stage sampling design. It was shown that indirect change estimation is prone to large bias. In *paper II*, HY was found to be a very precise

estimator for change. The simulations confirmed its precision, but exposed biases of up to 75% which depreciated the benefits of using ALS in terms of accuracy in most strata. In the absence of a geographical trend in AGB and AGB change, the systematic sampling design had a minimal effect on the sampling variance, and the variance estimators were not always conservative.

Synopsis

1. Introduction

Forests are an indispensable resource. From an anthropocentric perspective, the roles of forests range from our basic subsistence to increasing the comfort of our daily lives. For this reason, decision makers starting from forest managers to government agencies and international regulatory bodies are committed to sustainability. Having been identified as a major carbon sink (Pan et al. 2011), the forests could play a key role in climate change mitigation given the international commitment to reduce greenhouse gasses emissions (IPCC 2014). Making sensible decisions rely on timely and accurate information about the forests at different spatial scales. Most developed countries have well-established national forest inventories (NFIs), which typically consist in countrywide field surveys (Tomppo et al. 2010). Field based estimates are commonly used as information for policy makers, or reporting under international commitments (e.g. Kyoto Protocol). While the national forest inventory surveys were designed to be adequately accurate for countrywide estimates, the relatively small sample size at the level of smaller regions, may not meet precision requirements. Increasing the sampling intensity is not practical, due to the costs. In developing countries, the cost of intensive field based inventory may be temporarily worthwhile but this approach could be prevented by poor infrastructure and inaccessibility. These impediments apply to remote regions and inaccessible areas of developed countries as well. The feasible alternative in these situations is to support the surveys with remotely sensed data. Remote sensing may reduce the cost of forest surveys and increase the precision of the estimated parameters. Tomppo et al. (2008) give a review of how NFIs are enhanced with remotely sensed data.

1.1. LiDAR assisted forest surveys

Among the remote sensing technologies, lasers have earned a special prestige in forestry. In the past few decades we have learned their excellent ability to characterize the vertical structure of the forests, and thus carry abundant information on numerical parameters such as above ground biomass, mean canopy height, or standing wood volume, but also qualitative characterization of ecological parameters (Coops et al. 2016; Lone et al. 2014). First lasers were tested in the early 60s and like most of the technological exploration in the cold war era, work advanced in parallel on both sides of the iron curtain. Nelson (2013) gives an insightful historical account of laser development from the early days when the vegetation laser returns were seen as noise that ought to be removed rather than useful information to the first successful experiments using laser profiling to predict timber volume (Maclean and Krabill 1986) or biomass (Nelson et al. 1988).

Area based methods with airborne laser scanning (ALS) surveys have seen the most operational success (Koch 2010; Næsset et al. 2004; Næsset 2014; Zolkos et al. 2013). The general methodology was initially proposed by Næsset (1997). It entails tessellation of the area of interest into units that typically match the size of the field plots. For every unit, a set of ALS metrics is computed from the georeferenced point cloud of laser echoes. Georeferenced field plots are the basis of determining the relationship between ALS metrics and the variable of interest, a relationship that is subsequently generalized over the area of interest using parametric and nonparametric methods (Gagliasso et al. 2014).

The acquisition cost of ALS remains relatively high. With increased size of areas of interest, the cost efficiency of wall-to-wall ALS surveys is hampered by high acquisition costs relative to the gain in precision (Ene et al. 2016a). ALS sampling has been suggested as a cost effective alternative (Næsset 2005; Wulder et al. 2012). Given the airborne platform of acquisition, the natural way to collect ALS samples is along narrow corridors. One way to carry out partial acquisition of ALS is by strip sampling. This approach has been trialed in several different large-area surveys: Hedmark County, Norway – 27390 km^2 (Gobakken et al. 2012; Næsset et al. 2013b), western lowlands of the Kenai peninsula – 9400 km^2 and upper Tanana valley – 2012 km^2 in Alaska, USA (Andersen et al. 2009; Andersen et al. 2011), and Liwale District, Tanzania - 15867 km^2 (Ene et al. 2016b). In Maltamo et al. (2016) ALS data was acquired along a 1500 km long north-south transect spanning most of Norway. In the context of laser sampling, laser profiling has also seen renewed interest (Nelson et al. 2012). The parameter of interest in all of these studies was forest biomass, or more precisely above ground biomass. Information about the stocks of forest biomass is important for at least two reasons. First, forest biomass is a robust proxy for carbon (i.e. about 50% content), and second for its energetic value (e.g. Andersen et al. (2011)). Repeated acquisition of ALS samples over large areas opened the opportunity to investigate the change in forest biomass (Ene et al. 2017; Strîmbu et al. 2017).

1.2. Estimation and uncertainty

The Kyoto Protocol signatories have committed to report the carbon stock changes yearly. Unbiasedness, transparency and consistency are some of the so called good practices that should guide the process (IPCC 2006). Uncertainty is of central concern (Frey et al. 2006) and should be approached rigorously under sound statistical inference (Gregoire et al. 2016a; Magnussen et al. 2014).

Design-based (DB) and model-based (MB) are two inferential paradigms that assert different sources of estimation uncertainty. In DB inference, uncertainty originates in the sampling variability, whereas in MB inference, the uncertainty in the model parameters induce uncertainty in the estimates. DB inference relies on the properties of a probability sample, therefore a probability sample is essential, whereas for MB is not. In MB, sampling is intended for estimating the parameters of the so called superpopulation model. In this case nonprobability sampling such as purposely sampling is just as valid (Royall 1970). DB inference extrapolates properties of a sample that is random to the entire population that is fixed. MB views the population as random, or better said as a random realization of the superpopulation described by a model whose parameters are fixed. For a revelatory discussion on the differences between DB and MB inference see Gregoire (1998).

Estimation frameworks are constructed on the theoretical foundation provided by the two inferential philosophies. For ALS sampling surveys, two such frameworks have been advanced: a two-stage model assisted framework (MA) (Gregoire et al. 2011) and a two-phase hybrid framework (HY) (Ståhl et al. 2011). The MA framework lays exclusively in the DB inference. Both stages of sampling are probabilistic, and are subject to sampling error. In two-stage sampling, the population is partitioned into primary sampling units (PSU), and each PSU consists in a set of secondary sampling units (SSU). The first stage of sampling selects a sample of PSUs, and the second stage subsamples SSU within each PSU selected in the first stage. The ALS strips correspond to PSUs and the field plots to SSUs. Since the two stages of sampling are independent, the variance estimated within the MA framework adds two components: the variance due to the first stage sampling and variance due to the second stage sampling. Both components depend on the sampling design in their respective stage, being a consequence of how much the estimated parameter of interest (i.e. mean AGB) varies across all the possible first stage samples, respectively across all the possible second stage samples. At the basis of the MA framework is the so-called difference estimator (Särndal et al. 1992, p. 222) that works by adjusting a rough but informed prediction across population elements by the differences observed in probability sample. In the case of two-stage MA estimation, synthetic predictions are made at the level of the first stage sample, where auxiliary data are available, followed by adjustments within each PSU based on the subsampled SSUs. The HY framework combines the properties of the probabilistic sample in the first phase, with the properties of the model in the second phase. Just as with the MA framework the estimate variance adds two independent components, the first being a consequence of the variation between all possible samples of auxiliary data, and the second a consequence of uncertainty in the model that links the auxiliary variables (e.g. ALS) with the variable of interest (AGB). Here model uncertainty refers strictly to uncertainty in model parameters since the residual error can be ignored when estimating parameters of a large population (Ståhl et al. 2011). The estimation is entirely synthetic and does not involve field sampling (except when the model parameters are estimated, a process typically assumed to be external). With exclusive reliance on the model, HY estimation (and MB in general) is under an inherent risk of estimation bias. Ståhl et al. (2016) illustrates the roles of models in different estimation frameworks including hybrid estimation. Since the initial publication of the two estimation frameworks a certain amount of experience has been gained with inference following ALS sampling. Several new estimators have been developed, in particular within the MA framework. Ringvall et al. (2016) used a ratio estimator in the first stage of sampling, with the ALS strip size as auxiliary, and added covariance terms between estimates from different post-strata (similar to the HY estimator proposed by Ståhl et al. (2011)). Gregoire et al. (2016b) improved the second stage variance estimation, by conditioning on the sample size in the second stage of sampling. This also introduces covariance terms in post-stratified estimation, as for a fixed second stage sample size the number of field plots falling within a post-stratum is inversely correlated with the number of plots that fall within the other post-strata. Saarela et al. (2017) introduced a new variance estimator that uses the auxiliary information to a greater extent and showed that it was more stable that a traditional Horvitz-Thompson MA estimator (i.e., the variance of the estimated variances was smaller).

Change following repeated ALS surveys was studied in several smaller scale surveys with repeated wall-to-wall ALS acquisition (Bollandsås et al. 2013; Magnussen et al. 2014; Magnussen et al. 2015; McRoberts et al. 2015b; Næsset et al. 2013a; Økseter et al. 2015; Skowronski et al. 2014). These studies show two approaches to change estimation. Change can be estimated directly with a single variable of interest representing the difference in AGB between two points in time, or indirectly by estimating the AGB stock separately for each time instance, and subsequently taking the difference of the two estimates. McRoberts et al. (2015b) explores several ways to model change. Indirect change estimation has the advantage of enabling reporting AGB change that is consistent with individual stock values (i.e. single-time estimates). The same estimation frameworks described above may be used for change estimation following repeated ALS strip sampling.

1.3. Simulations

Assessing the statistical properties of these estimators, among which those related to estimation uncertainty, are of prime concern. This however proves to be an intricate task, as multiple deviations from the theoretical assumptions upon which the estimators are constructed amount to a complexity that is not easily captured analytically. A feasible alternative is to perform Monte Carlo simulations, by exploring the space of all possible estimation inputs empirically. The credibility of a simulative approach stands in the quality of the artificial simulation environment and how accurately the domain of possible inputs is defined. In assessing estimators, the simulation environment is typically an artificial population, and the input domain is dictated by a sampling design. The level of detail in the artificial population must be appropriate for the objective of the simulations (i.e., the particular effect under investigation). For instance, simulating a simple random sampling strategy would not require a spatially explicit forest population. Kangas et al. (2016) performed simulations on a spatially inexplicit copula population to investigate the effect of internal versus external models in estimation. In this case, the only important aspect of the artificial population was the multivariate relationship between different variables, a property secured by modeling the multivariate relationship with copula functions. When for instance the sampling design effect is under inquiry, a spatially explicit population is required. Grafström and Ringvall (2013) investigated the possibility to use auxiliary data to balance the field samples both spatially and in the auxiliary space. For this purpose, the authors performed sampling simulations on a small population of 846 observations coming from a dense field inventory. Grafström et al. (2014) further investigated the new sampling technique with improved simulations on an artificial surrogate of 30 000 ha area in Kuortane, Finland. The forest population was generated with a method pioneered in Ene et al. (2012), where the multivariate variable relationship was modeled with copula functions, and then a copula sample of observations was generalized on a wall-to-wall auxiliary using nearest neighbor (NN) imputations. The technique has since been used in several forest survey simulations. Using this artificial population generation technique, several multi-step modeling techniques for model-based inference (Saarela et al. 2016), as well the prediction-based variance estimator for MA estimation (Saarela et al. 2017), were validated. Both innovations were relevant for large-area forest survey. Using similar simulation methods, Saarela et al. (2015) investigated the effects of sample size, model form, and model parameter covariance matrix estimation on the accuracy of model based estimators. The copula technique expands a relatively small set of observations to a population of arbitrary size while maintaining the integrity of the multivariate relationship between population variables. Furthermore, performing NN imputations preserves the general geographical trend in the population as defined by the wall-to-wall covariates. An aspect that has not been addressed is the short-range autocorrelation of proximal population units, which can further expose the design effect of certain sampling strategies. In addition, methods to create realistic change populations are needed to assess MA and HY estimators of change. In general, more experience with large-scale change estimation is needed as a prerequisite to devise robust estimation strategies to be used operationally.

1.4. Research objectives

The broad objective of this thesis was to investigate large-area forest biomass stock and change estimation supported by ALS sampling. To this end, assessing the performance of MA and HY estimators was an important goal. A particular objective was to develop simulation methodologies necessary in assessing complex forest surveys.

The thesis comprise three scientific papers, with the following individual objectives:

Paper I: *Spatially consistent imputations of forest data under a semivariogram model*

The objective was to develop a method to perform NN imputations of spatial data that conform to a prescribed semivariogram model, as well other prescribed distributional properties (e.g. mean or histogram). This was the basis of the methodology to generate complex change population used as support for simulations in *paper III*.

Paper II: *Post-stratified change estimation for large-area forest biomass using repeated ALS strip sampling*

The main objectives of this study was to investigate post-stratified model assisted and hybrid change estimation. Specific objectives were to test a nested post-stratification scheme by cover class and change class, and to assess parametric bootstrapping as a simulative approach to estimate the model uncertainty component in hybrid estimation.

Paper III: *Simulative assessment of model assisted and hybrid estimation of change using repeated ALS sampling*

This study had two objectives: (i) to develop a methodology to construct spatially explicit change populations with prescribed properties tailored to an area of interest, and (ii) asses model assisted and hybrid estimators by sampling simulations.

2. Materials

2.1. Study areas

The materials in this thesis were acquired from two study areas: a 852 ha forest in the municipality of Våler, and the southern portion of Hedmark County spanning 9758 km^2 (Figure 1). Both areas are located in southeast Norway, a region with some of the most productive forests in the country, and therefore subjected to intense forest management. The tree species composition here is typical to the boreal forests of the Nordic countries with relatively low diversity. Norway spruce (*Picea abies* (L.) Karst.) and Scots pine (*Pinus sylvestris* L.) dominate the landscape. Birch (*Betula pubescens* Ehrh.) is the only deciduous with a somewhat noteworthy presence.

Figure 1. Study areas location within Norway. In Våler, grey lines delineate forest stands, small black dots are the stand-wise inventory plots, and hollow circles are the systematic field survey. In Hedmark, dots indicate the locations of NFI plots and the white strips constitute the ALS survey.

2.2. Field data

In Våler, two independent field surveys were carried out in 2010 (Table 1). A systematic survey, with 177 plots laid out on a 150 m × 150 m grid, and a more intense survey with 923 plots in a subset of the forest stands (12 plots per stand on average). The size of these plots varied with the forest type from 80 m^2 (see Table 1 note) to 400 m^2. For a more detailed description of Våler survey see Næsset et al. (2013a).

In Hedmark, the field survey was provided by the Norwegian NFI (Tomter et al. 2010). The NFI permanent circular plots have a fixed area of 250 m^2, and are laid in the nodes of a 3 km × 3 km grid. According to the longitudinal survey protocol, a fifth of the plots are revisited yearly, which results in five years inventory cycles. In our study, we used 316 plots (Table 1) measured once in 2005, 2006 and 2007 (during the 9th inventory cycle), and then again in 2010, 2011 and 2012 (10th inventory cycle).

Table 1. Field survey summary.

Forest/cover class	Area (m^2)	Count	Mean AGB ($Mg{\cdot}ha^{-1}$)	Area (m^2)	Count	Mean AGB ($Mg{\cdot}ha^{-1}$)
Hedmark		2006			2011	
Nonproductive - Nonforest	250	71	16.42	250	71	17.94
Young	250	90	31.28	250	90	41.90
Low productive	250	46	48.64	250	46	51.40
Medium productive	250	63	111.81	250	63	119.94
High productive	250	46	129.62	250	46	135.64
Våler		Systematic survey			Stand survey	
Recently regenerated	80*	23	5.03	80*	178	5.79
Young	400	42	112.32	125	244	108.75
Mature spruce-dominated	400	62	150.11	250	437	152.17
Mature pine-dominated	400	50	162.49	250	64	121.32

Note: * cluster of 4 subplots, 20 m^2 each

2.3. Remotely sensed data

Satellite imagery and ALS data were used throughout the thesis. The satellite data consisted in freely available Landsat 5 (Hedmark) and 7 (Våler) products (Table 2). In Våler, ALS data were acquired for the entire area. In Hedmark, the ALS survey comprised a sample of east-west parallel strips that covered only around 8% of the whole region. The strips were approximately 500 m wide and spaced 6 km apart, centered on every second row of NFI plots (Figure 1 b). In 2006, 53 strips were scanned across the entire county. Five years later, unfavorable weather conditions led to a less successful acquisition campaign with only the southmost 24 strips being reflown, in the vegetative seasons of 2011 and 2012. As the focus here was on AGB change estimation, we were constrained to use only the 24 overlapping strips, and to restrict the extent of the study area accordingly. The essential acquisition parameters for the ALS surveys are summarized in Table 3. In addition to the raw remotely sensed data we used a land cover classification derived from official AR5 land use maps (Bjørdal and Bjørkelo 2006), digital terrain models, and Landsat 5 images.

Table 2. Satellite imagery

Parameter	Våler	Hedmark
Sensor	Landsat 7 ETM+	Landsat 5 TM
Resolution	30 m	30 m
Date	3 June 2010	3-10 June 2007

Table 3. ALS datasets

Parameter	Våler	Hedmark 2006	Hedmark 2011
Laser scanner	Optech ALTM Gemini	Optech ALTM 3100	Leica ALS70
Pulse density (m^{-2})	7.3	2.8	~5
Date	2 July 2010	22 July 2006 – 16 September 2006	4 August 2011 – 24 September 2011 29 August 2012 – 30 September 2012
Extent	Wall-to-wall	53 strips	24 strips

3. Methods

3.1. Data processing

AGB values were predicted for individual trees using field measurements and allometric models (Marklund 1988), then aggregated at the plot level and scaled to $Mg \cdot ha^{-1}$. The satellite imagery were atmospherically corrected and resampled using bilinear interpolation to an appropriate pixel size to match the field plot area. In Våler, since the plot sizes were between 80 m^2 and 400 m^2, a compromise was made with a pixel size of 15 m (225 m^2), which was close to the average plot size. In Hedmark, the NFI plots had a standard size of 250 m^2, which corresponded to a pixel size of 15.81 m. In Våler, the near infrared and red bands were used to compute the normalized difference vegetation index (NDVI). In Hedmark, the first four bands (red, green, blue, and near infrared) were used as support to create the forest population (*Paper III*). Here, the satellite imagery also assisted, along existing land use and topographic maps, in classifying the area into land cover classes. Originally, there were eight such classes (Gobakken et al. 2012), four of which were merged as constrained by the small number of field plots. The five resulting cover classes were: (1) nonproductive-nonforest, (2) young forest, (3) low, (4) medium, and (5) high productive forest. Basic processing of the ALS data was performed by the contractors (Blom Geomatics and Terratec), followed by ground surface reconstruction using the Triangular Irregular Network densification algorithm (Axelsson 2000), point cloud normalization, and building removal. Finally, the ALS point clouds were tessellated, just as the satellite images, with cell sizes of 15 m (Våler) and 15.81 m (Hedmark). In each cell, height and density variables were computed as described in Gobakken et al. (2012). The height percentiles are denoted by h_{10}, h_{20}, …, h_{90}, the mean and maximum height by h_{mean}, h_{max}, and the density metrics by d_{10}, d_{20}, …, d_{90}. In Hedmark, the raw ALS strips were cropped out to a width of 500 m together with portions that did not overlap between the two acquisition times. This ensured that all ALS observations had ALS metric values for both points in time.

3.2. Spatially optimized imputations

The wall-to-wall ALS together with the dense field survey in Våler recommended this dataset as an excellent support to investigate the spatial autocorrelation of forest and variables from remotely sensed data. This dataset was used in *paper I* to develop the methodology to optimize nearest neighbor imputations with respect to spatial and distributional properties.

The methodology builds upon Barth et al. (2009), who demonstrated the use of simulated annealing to perform what they called spatially consistent imputations. The authors used simple measures of autocorrelation that quantify the relationship of adjacent units (pixels). We extended the notion of spatial consistency to the more general parameters of a semivariogram, which quantify the spatial relationship of observations at arbitrary distances apart. In addition, our methodology controls the distribution of the imputed observations with the help of a target histogram.

First, semivariogram models were fitted to the empirical observations at the field plot level, to analyze the spatial autocorrelation of an ALS metric (h_{40} – the variable most correlated with AGB), the NDVI derived from the satellite image, and AGB. Several experiments were performed (Figure 2) with variables changing roles between carrier and reference, and using different objective functions. First, h_{40} was imputed on the NDVI carrier (Figure 2, a). Having complete control of the true parameter values of the h_{40}population, which was available wall-to-wall, we were able to compare the imputation results obtained with the new method to those obtained using Barth et al. (2009), and to the “ground truth”. NDVI to AGB

(Figure 2, b) and h_{40} to AGB (Figure 2, c) imputation were also performed, to test real scenarios where AGB is the variable of interest and when the carrier is a poor, respectively good predictor for AGB.

Every unit in the carrier was initially assigned k possible elements from the reference set of observations, based on a proximity measure in the feature space of the carrier (the k NNs). We used a simulated annealing algorithm to select one of the k NNs per carrier unit, assisted by an objective function. The objective function is a measure of distance from an arbitrary solution to the desired solution, in this case quantifying the difference between a given semivariogram and histogram and their respective targets. For the semivariogram this distance was calculated as:

$$O_{SV} = \sum_{i=1}^{n} \frac{|SV(h_i) - SV_{tg}(h_i)|}{SV_{tg}(h_i)}$$

where n is the number of lag distances, $SV(h_i)$ is the semivariation at distance h_i and $SV_{tg}(h_i)$ is the target semivariation at distance h_i. The histogram distance was calculated as:

$$O_H = \sum_{i=1}^{n} \frac{|H(i) - H_{tg}(i)|}{H_{tg}(i)}$$

where n is the number of histogram bins, and $H(i)$ and $H_{tg}(i)$ are the number of observations, respectively target number of observations in the i-th bin. The objective function was constructed by adding components corresponding to each parameter. In *paper I*, we tested different objective functions:

$$O_{(1)} = O_{SRV} + O_{Corr} + O_{\mu}$$

$$O_{(2)} = O_{SV} + O_{\mu}$$

$$O_{(3)} = O_{SV} + O_H$$

where $O_{(1)}$ corresponds to Barth et al. (2009) with targets for three variables: short range variance (SRV), adjacent pixel correlation, and the population mean. The SRV was defined as the average variance of observations in 3×3 pixel windows. The objective components of these parameters have only one term, e.g., $o_{\mu} = \frac{|\mu - \mu_{tg}|}{\mu_{tg}}$. The method was implemented in a Java application that allows the user to parametrize and visualize the optimization process.

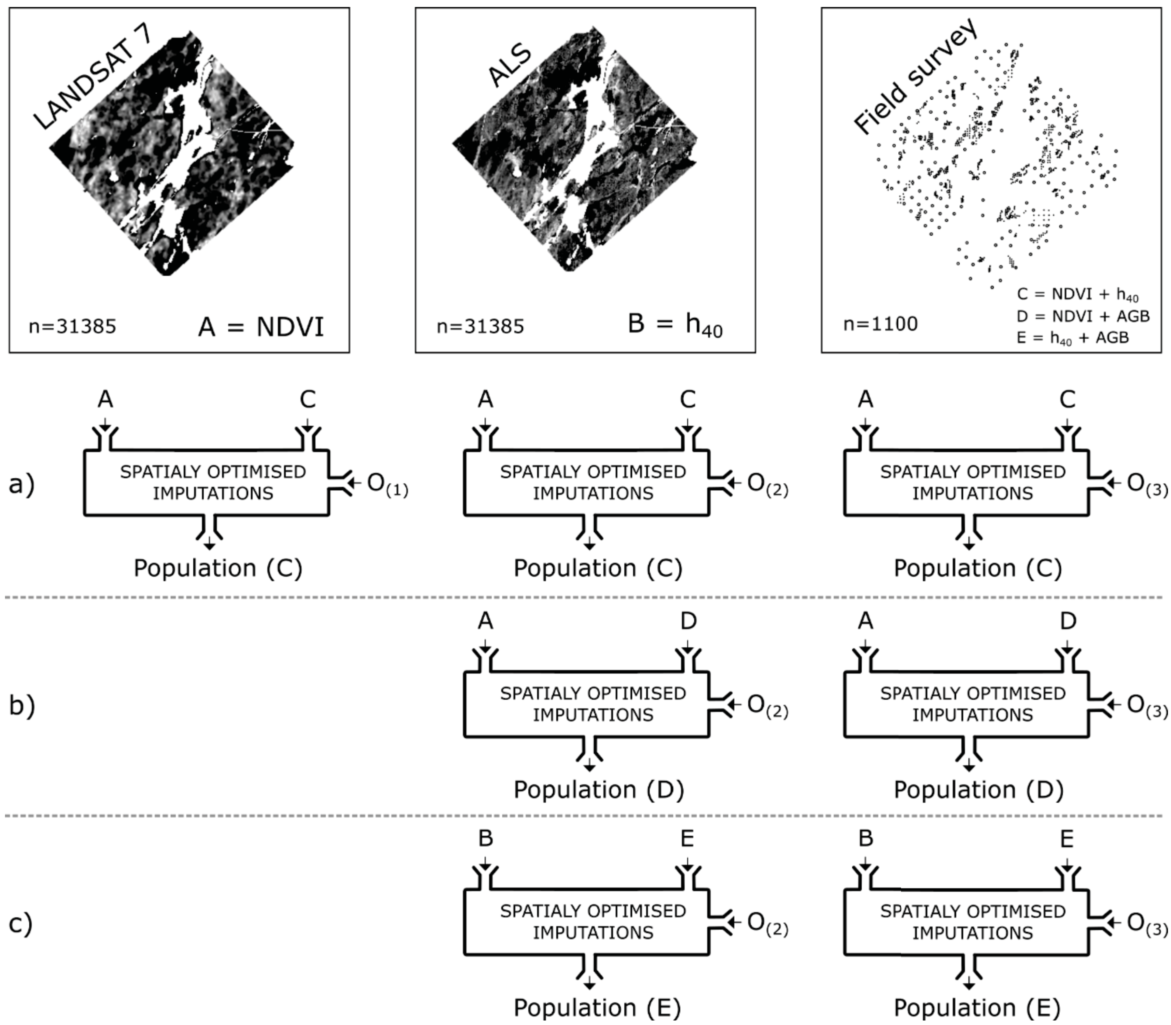

Figure 2. Overview of the experiments in *paper I*.

In *paper III*, $O_{(2)}$ was used as objective function to construct the artificial population. Here the population was generated in two stages of imputations (Figure 3). First, the ALS population was generated with the support of the Landsat 5 images, then the AGB population on the wall-to-wall ALS carrier generated in the previous stage. The reference set for the ALS imputations consisted in real observations sampled from the ALS strip survey data, and in the second stage of imputations, the reference consisted in synthetic observations generated with a copula approach.

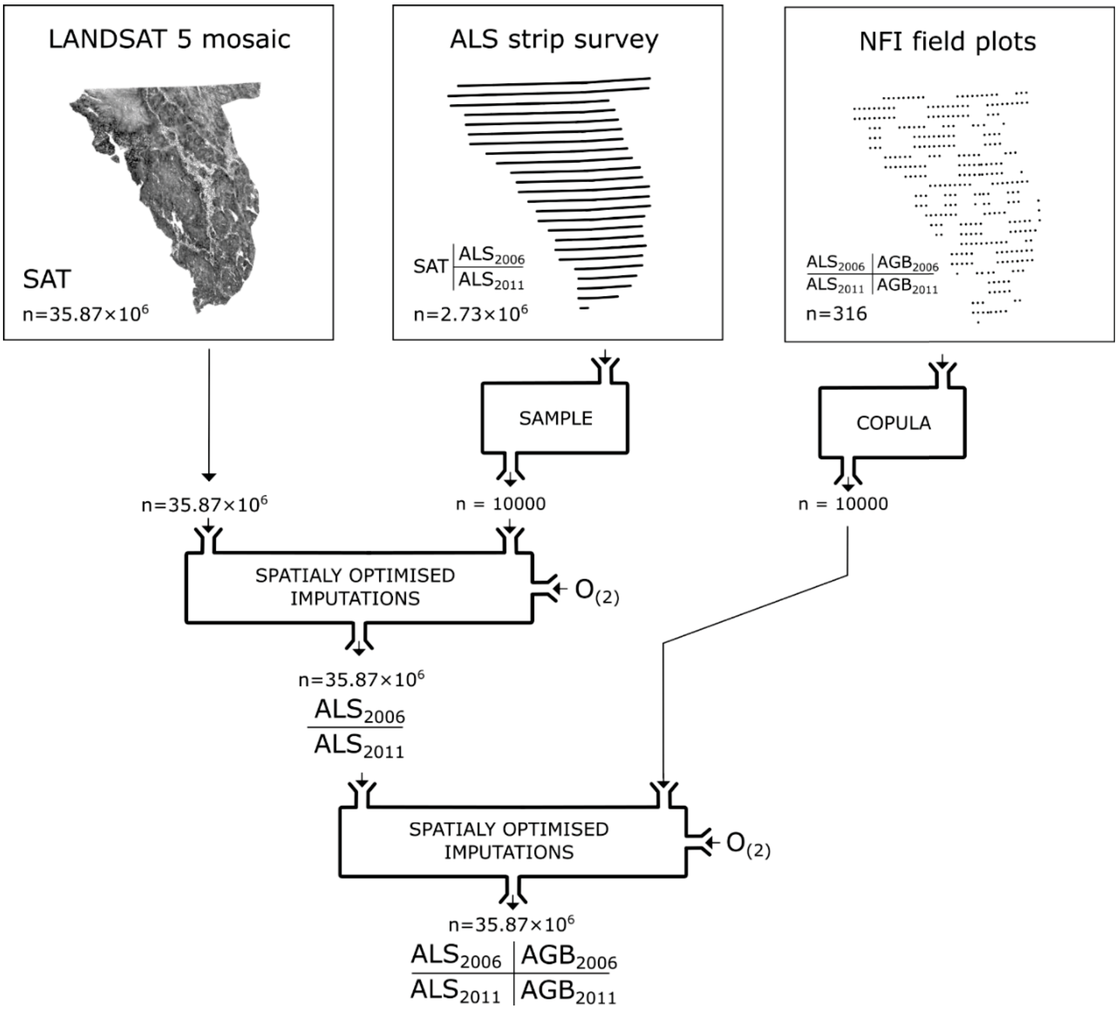

Figure 3. Summary chart of the artificial population in Hedmark. A more detailed chart is shown in Figure 1, *paper III*

3.3. Models

Two types of models were used throughout the thesis: semivariogram models and predictive models for AGB. For the semivariograms, exponential (*paper I*) and powered exponential (*paper III*) models were used:

$$SV(h) = \sigma^2 \left(1 - e^{-\left|\frac{h}{\varphi}\right|^p}\right)$$

Where h is the lag distance, σ^2 is the sill, φ is the range parameter, and p is the power parameter (in *paper I*, $p = 1$). The semivariogram parameters were estimated directly by ordinary least squares fitting to empirical semivariances where possible (i.e. remotely sensed data, or the dense field survey in Våler), or indirectly, by using the sample variance as proxy for the sill (Barnes 1991) and borrowing parameter values that were fitted to a correlated variable (i.e. AGB semivariograms in Hedmark). The semivariogram analyses were performed with the R package geoR (Ribeiro and Diggle 2016).

The ALS-AGB relationship was modeled within the frameworks of ordinary least squares (OLS) and generalized least squares (GLS) using time-invariant models (Magnussen et al. 2015). Predictors and the response variables were log transformed to linearize their relationship. The models were selected using backward and best subset methods with Bayesian information criterion (BIC), and mindful of the variance inflation factor. During the selection phase, parameters were fitted using OLS to admit likelihood tests. Finally, the coefficients of the selected model were refitted using GLS with a compound symmetrical covariance structure to account for the longitudinal correlation between observations (i.e. measurements in 2006 and 2011 on the same plot). Stratum specific models were selected and fitted in each cover class:

$$\hat{y}_h = f_h(\widehat{\boldsymbol{\beta}}_{\boldsymbol{h}}, \boldsymbol{x})$$

where h is the cover class, $\widehat{\boldsymbol{\beta}}_{\boldsymbol{h}}$ is the vector of estimated coefficients, and $\boldsymbol{x}$ is the vector of predictors (i.e. ALS metrics).

3.4. Estimation

MA and HY estimators were used to estimate AGB stocks and change. For change, the indirect approach was adopted (McRoberts et al. 2015b), by which change is derived by the difference in AGB stocks estimated separately for the two times. Both MA and HY are ratio estimators, as per Ringvall et al. (2016) and Ståhl et al. (2011), with the ALS strip area used as auxiliary. Mean AGB was estimated by

$$\hat{\mu}_{MA} = \frac{\sum_{i=1}^{m}\left[\sum_{k=1}^{N_i}\hat{y}_{ki} + \frac{N_i}{n_i}\sum_{k=1}^{n_i}(y_{ki} - \hat{y}_{ki})\right]}{\sum_{i=1}^{m} A_i}$$

$$\hat{\mu}_{HY} = \frac{\sum_{i=1}^{m}\left[\sum_{k=1}^{N_i}\hat{y}_{ki}\right]}{\sum_{i=1}^{m} A_i}$$

where m is the number of ALS strips, N_i is the number of cells in strip i, n_i is the number of field plots in strip i, y_{ki} and $\hat{y}_{ki}$ are the observed, respectively predicted AGB values in the k-th field observation within strip i, and A_i is the area in hectares of strip i. The variances of $\hat{\mu}_{MA}$ and $\hat{\mu}_{HY}$ add two components that correspond to independent sources of variation:

$$\widehat{Var}(\hat{\mu}_{MA}) = \widehat{Var}_{S1}(\hat{\mu}_{MA}) + \widehat{Var}_{S2}(\hat{\mu}_{MA})$$

$$\widehat{Var}(\hat{\mu}_{HY}) = \widehat{Var}_{S1}(\hat{\mu}_{HY}) + \widehat{Var}_{M}(\hat{\mu}_{HY})$$

In the case of MA, the two sources of variation are due to the two stages of sampling: strip sampling ($S1$), and the subsample of field plots ($S2$). For HY, the strip sampling ($S1$) in the first phase and the model uncertainty (M) in the second phase. With post-stratification, the estimates of mean and variance are calculated separately for each post-stratum using the above equations. The overall estimates across stratum means and variances are calculated by:

$$\hat{\mu}_{MA} = \boldsymbol{W}^T \boldsymbol{\hat{\mu}_{MA}}$$

$$\hat{\mu}_{HY} = \boldsymbol{W}^T \boldsymbol{\hat{\mu}_{HY}}$$

where $\boldsymbol{W}$ is the vector of post-stratum proportions, and $\boldsymbol{\hat{\mu}_{MA}}$ and $\boldsymbol{\hat{\mu}_{HY}}$ are vectors of estimated mean AGB in each post-stratum. Because of ALS strips intersecting several post-strata, the per-stratum estimates are not independent, which means that variance estimators for the across stratum means must account for the covariances within $\boldsymbol{\hat{\mu}_{MA}}$ and $\boldsymbol{\hat{\mu}_{HY}}$:

$$\widehat{Var}(\hat{\mu}_{MA}) = \boldsymbol{W^T} \widehat{\boldsymbol{Cov}}_{MA} \boldsymbol{W}$$

$$\widehat{Var}(\hat{\mu}_{HY}) = \boldsymbol{W^T} \widehat{\boldsymbol{Cov}}_{HY} \boldsymbol{W}$$

where $\widehat{\boldsymbol{Cov}}_{MA}$ and $\widehat{\boldsymbol{Cov}}_{HY}$ are the estimated covariance matrices for $\boldsymbol{\hat{\mu}_{MA}}$ and $\boldsymbol{\hat{\mu}_{HY}}$. Just as before, they are composed of two components:

$$\widehat{\boldsymbol{Cov}}_{MA} = \widehat{\boldsymbol{Cov}}_{S1} + \widehat{\boldsymbol{Cov}}_{S2}$$

$$\widehat{\boldsymbol{Cov}}_{HY} = \widehat{\boldsymbol{Cov}}_{S1} + \widehat{\boldsymbol{Cov}}_{M}$$

where $\widehat{\boldsymbol{Cov}}_{S1}$, $\widehat{\boldsymbol{Cov}}_{S2}$, and $\widehat{\boldsymbol{Cov}}_{M}$ are covariance matrices for the first stage sampling, second stage sampling, and model uncertainty. These constructs offer a generalized framework for post-stratified two-stage MA and two-phase HY estimation. The primary stratification scheme was by land cover classes and it was used in *papers II* and *III*. In *paper II*, a nested post-stratified scheme was trialed, by both cover class and change class. The change classes were established based on the ALS metrics from both times and represented four simple categories: unchanged forest (laser echoes above 1.3 m in both times), clear felled forest (laser echoes above 1.3 m in 2006 but not in 2011), regenerated forest (laser echoes above 1.3 m in 2011 but not in 2006), and unchanged nonforest (no laser echoes above 1.3 m in either times). In this thesis, only $\widehat{\boldsymbol{Cov}}_{S1}$ was always a proper covariance matrix with nonzero elements. $\widehat{\boldsymbol{Cov}}_{S2}$ was diagonal because the second-stage sample was assumed to be independently selected in each post-stratum. $\widehat{\boldsymbol{Cov}}_{M}$ was either diagonal with post-stratification by cover class since models were selected and fitted independently in each cover class, or block diagonal when the post-stratification scheme nested cover and change classes. The estimation precision was reported in terms of the more intuitive standard error: $\widehat{SE}(\hat{\mu}) = \sqrt{\widehat{Var}(\hat{\mu})}$.

To assess the relative gain in precision or accuracy with ALS as auxiliary data, Horvitz-Thomson (HT) (Horvitz and Thompson 1952) estimates were computed using the field plots only. Relative efficiencies (RE) were calculated for the analytically estimated standard errors ($RE_{\widehat{SE}} = \frac{\widehat{SE}(\hat{\mu}_{HT})}{\widehat{SE}(\hat{\mu}_{MA\ or\ HY})}$). In *paper III*, the observed standard error ($SE(\hat{\mu}) = \sqrt{Var(\hat{\mu})}$) and the observed root mean square error ($RMSE(\hat{\mu}) = SE(\hat{\mu}) + Bias(\hat{\mu})$) were calculated following sampling simulations. With respect to these, two other REs were calculated: $RE_{SE} = \frac{SE(\hat{\mu}_{HT})}{SE(\hat{\mu}_{MA\ or\ HY})}$ and $RE_{RMSE} = \frac{RMSE(\hat{\mu}_{HT})}{RMSE(\hat{\mu}_{MA\ or\ HY})}$. Values greater than one of the RE indicate a gain in precision (or accuracy for RE_{RMSE}) with the ALS survey.

3.5. Simulations

A major focus of this thesis was the simulative approaches intended to complement theoretical derivations or offer an alternative when the latter are not feasible. In *paper II*, parametric bootstrapping was demonstrated as an alternative to estimate the uncertainty due to the model, and in *paper III* sampling simulations were performed to assess the estimators' properties, and compare their performance and adequacy for different types of estimation.

With parametric bootstrapping the effect of the uncertainty in model coefficients was simulated by repetitively sampling from the multivariate distribution of the model coefficients, recalculating the predictions and the HY estimates according to each sampled set of coefficients, and finally analyzing the distribution of the estimates. Simply put, parametric bootstrapping was used as an empirical method to estimate $\widehat{\boldsymbol{Cov}}_{M}$.

Sampling simulations in *paper III* were performed according to the real Hedmark survey, rather than the theoretical two-stage sampling design. The difference is that in theory, the primary sampling units are selected first (i.e. the ALS strips), and then a subsample of secondary units (field plots) are selected in a second stage. In reality however, the NFI plot grid was established prior to the ALS flight campaigns, thus conditioning the latter survey.

4. Results and discussion

4.1. Spatially optimized imputations

The method proposed in *paper I* proved to be efficient. The population semivariogram converged to the desired model in most cases (Table 4), and it was time efficient despite its complexity. Spatially optimizing the imputations also had the effect of improving the prediction error (NDVI to h_{40} imputations), which was something we did not explicitly aim for. The mean absolute error in predicted h_{40} decreased from 4.01 m to 3.63-3.69 m. This result should be further investigated as it may find applications in the domain of nonparametric estimation methods where recent efforts aimed to improve the k-NN technique to estimate forest parameters (McRoberts et al. 2015a; McRoberts et al. 2016). Convergence may be affected when the objective function is loaded with too many components (i.e. semivariance calculated for many lags, combined with multiple histogram bins; see semivariogram convergence with $O_{(3)}$ in Table 4). The methodology to generate the artificial population in *paper III* was developed mindful of this result, and some measures of precaution were taken (i.e. imputations in two steps, fewer lag distances for the semivariograms, and dropping the histogram objective). The results in *paper III* demonstrated that is possible to construct artificial forest populations with prescribed parameters for two points in time and complex multivariate and spatial properties. Figure 4 shows a small portion of the population generated with and without spatial optimization for comparison. In this thesis, the sole application of this methodology was in sampling simulations for evaluating estimators' properties. The spectrum of application is however wider. For instance, the field sampling effort can be optimized by balancing information with cost. This type of analysis has been done with sampling simulations (Grafström and Ringvall 2013; Grafström et al. 2014; Tokola and Shrestha 1999; Tomppo et al. 2014). The establishment of the Tanzanian NFI is a relevant example, where sampling simulations assisted in creating the NAFORMA clustered sampling design (Tomppo et al. 2014). Here among other design considerations, the number of plots per cluster and the distance between them could be adequately decided following sampling simulations, given an artificial population with a realistic spatial structure. Furthermore, realistic artificial populations with a consistent spatial structure may also be used in forest planning and forest scenario analysis, where it can be set as the initial state (Barth et al. 2009; Barth et al. 2012; Gustafson et al. 2000; Lämås and Eriksson 2003; Packalén et al. 2011).

Table 4. Spatial optimization results. Convergence is expressed as percentage of the distance travel from the initial state to the state at the end of the optimization with respect to the total distance from the initial state to the target (e.g., for unoptimized NN imputation convergence = 0%, and if it reached the target value for a parameter convergence = 100%). Bolded values correspond to parameters that were explicit in the objective function. * in *paper III* the convergence was >99% for all parameters, ALS metrics and AGB, in all strata, and for both points in time (2006 and 2011)

Imputation type	**Objective**	**Convergence (%)**		
		Semivariogram	Histogram	Mean
Våler experiments (*paper I*)				
	$O_{(1)}$	78.0	42.8	**100**
	$O_{(2)}$	**99.9**	47.5	**99.8**
	$O_{(3)}$	**93.8**	**100**	97.0
	$O_{(2)}$	**98.9**	35.3	**100**
	$O_{(3)}$	**94.8**	**99.8**	-58.0
	$O_{(2)}$	**99.1**	70.5	**100**
	$O_{(3)}$	**98.6**	**99.8**	83.8
Hedmark population generation (*paper III*)				
SAT to ALS	$O_{(2)}$	>99*	-	>99*
ALS to AGB	$O_{(2)}$	>99*	-	>99*

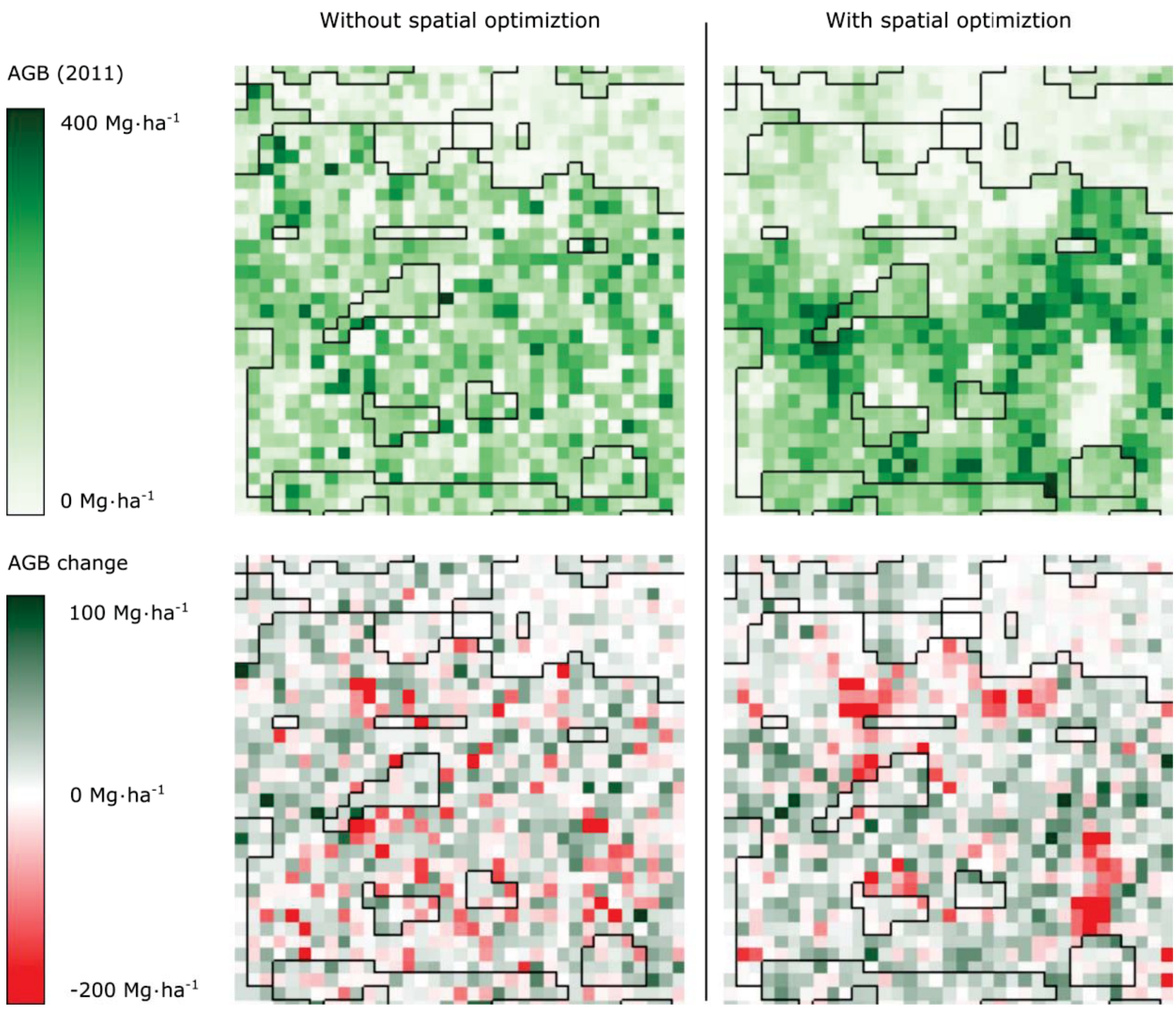

Figure 4. A small portion of the AGB population generated in *paper III*. The top images show the AGB population of 2011 and the bottom images are the change population obtained by subtracting 2006 AGB values from 2011 AGB values. Black lines delineate cover classes.

4.2. Biomass stock and change estimation

The results in *paper II* suggested a general positive trend in AGB change over the 5 years (Table 5). MA was more precise than HY for biomass stock estimation (i.e., single-time) and both MA and HY estimated change more precisely than HT, with HY outperforming MA for estimation within individual cover classes (Table 6). The proposed nested post-stratification scheme did not always improve the estimation precision (Table 6, $HY_{\times}$), but it retains its merits of enabling detailed reporting for change, according to cause of change within each post-strata. The four change classed in paper II were rather simple, as the main purpose was to demonstrate the nested post-stratification scheme. In addition, the change class sizes were disproportionate (e.g., clear felling and regeneration represented together less than 4% of the area sampled with ALS). A more advanced change class post-stratification, with more classes and balanced proportions could improve the estimation precision as well.

Table 5. Estimation summary (*paper II*). Units are Mg $\cdot$ha^{-1}

Time	MA		HY		HY$_\times$		HT	
	$\hat{\mu}_{MA}$	$\widehat{SE}(\hat{\mu}_{MA})$	$\hat{\mu}_{HY}$	$\widehat{SE}(\hat{\mu}_{HY})$	$\hat{\mu}_{HY\times}$	$\widehat{SE}(\hat{\mu}_{HY\times})$	$\hat{\mu}_{HT}$	$\widehat{SE}(\hat{\mu}_{HT})$
2006	69.1	2.03	67.6	3.12	69.3	3.35	58.4	2.81
2011	70.4	1.93	70.6	2.99	72.5	3.27	64.8	3.06
Change	1.36	0.81	3.05	0.90	3.18	0.92	6.38	1.65

Table 6. Relative efficiencies ($RE_{\widehat{SE}}$) of MA and HY estimators used with the Hedmark survey (*paper II*). Values > 1 are bolded and indicate an increase in precision relative to the direct estimation using field plots only. HY$_\times$ is the HY estimator with nested post-stratification by cover class and change class.

Time	Stratum	MA	HY	HY$_\times$
	Nonforest	**1.68**	**1.93**	**2.46**
	Young	**1.96**	0.84	0.86
	Low	0.94	0.82	0.93
	Medium	**2.22**	**1.36**	**1.37**
	High	**2.12**	**2.03**	**2.11**
	All cover classes	**1.39**	0.90	0.84
	Nonforest	**2.38**	**2.09**	**2.72**
	Young	**1.71**	0.85	0.86
	Low	**1.06**	0.89	**1.00**
	Medium	**2.23**	**1.67**	**1.66**
	High	**1.76**	**2.17**	**2.17**
	All cover classes	**1.58**	**1.02**	0.94
	Nonforest	**1.30**	**6.45**	**3.74**
	Young	**1.01**	**1.62**	**1.40**
	Low	**1.22**	**2.09**	**2.09**
	Medium	**2.48**	**2.68**	**2.69**
	High	**1.43**	**3.41**	**3.56**
	All cover classes	**2.04**	**1.83**	**1.79**

4.3. Simulations

4.3.1. Parametric bootstrapping

The results of parametric bootstrapping were consistent with the theoretical estimates of uncertainty due to the model. The empirically estimated $\widehat{\boldsymbol{Cov}}_M$ converged to its analytical counterpart within 1000 bootstrap samples (Figure 5). Demonstrating parametric bootstrapping had a twofold role: first as mutual validation with the theoretical HY estimator, and second, provide a viable alternative to isolate the model uncertainty effect when the analytical estimation becomes too complex (i.e., due to sampling design; multistage, post-stratification, etc.).

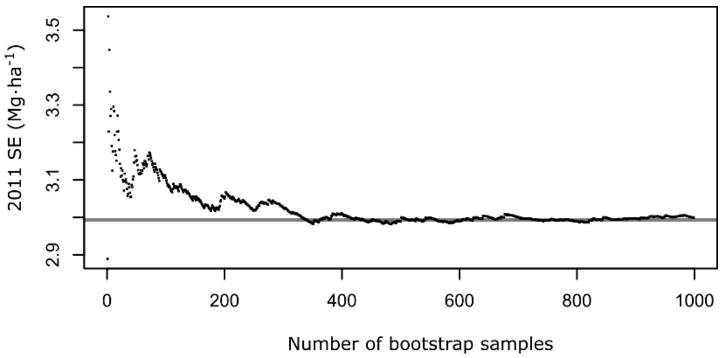

Figure 5. Parametric bootstrapping convergence of the empirically estimated $\widehat{SE}(\hat{\mu}_{HY})$ of the 2011 across-stratum estimates of mean AGB. The gray line is the analytically estimated $\widehat{SE}(\hat{\mu}_{HY})$

4.3.2. Sampling simulations

The sampling simulations in *paper III* revealed that bias can be a hindrance for indirect change estimation. Small bias in single-time estimates become large for change estimates, especially when change was small relative to the growing stocks. This is of particular concern with the HY estimation where biases of -2.69% to 8.34% for stratum-wise single-time estimates became in the range of -44.25% to 75.06% for change. For MA, the biases were between near 0% to 1.64% for single-time stratum-wise estimates, and -0.57% to 7.64% for change. The overall estimates of change with post-stratification had 0.36% bias with MA and -18.15% with HY. Without post-stratification, the bias of the overall change estimates was 0.07% with MA and -14.65% with HY.

Stratum-wise change was most precisely estimated by HY (Table 7, RE_{SE}). This was in accord with the findings of *paper II* (Table 6) where change was estimated with the original Hedmark survey data. The simulations reveal that the bias in HY estimation, annuls the benefits of the gain in precision in terms of accuracy. The north-south spatial trend was weak in South Hedmark. For change the already weak trend in AGB stocks effectively canceled out. As a result, the design effect of the systematic sampling was reduced. In fact, many variances were underestimated, notably by the MA estimator. The second stage of sampling also contributed to this result. First, because of the use of endogenous models which were shown to induce variance underestimation of MA estimators (Kangas et al. 2016). Second, due to the small number or lack of field plots per cover class and ALS strip. Among the simulated samples, 22% of the strip – cover class combinations had one or zero field plots. In these situations the second stage variance cannot be calculated and was set to 0 by default which resulted in underestimation of the second stage variance for the MA estimator. Future work should modify the estimators to handle these types of occurrence.

Post-stratification did not improve the overall across-strata estimation accuracy. This was especially true for estimates of change where the differences between the cover classes fade out. If the purpose of post-stratification is to increase the estimation precision, different post-stratification schemes should be employed (e.g., by criteria that differentiate change classes).

We end this discussion with a remark on the methods presented in Saarela et al. (2016), which offer a good example that would benefit from parametric bootstrapping as well as sampling simulations on a spatially consistent population. Saarela et al. (2016) proposed a MB estimator that utilizes three sources of information (e.g. wall-to-wall satellite, partial ALS, and field data) in two modeling steps. The methodology was also used in Puliti et al. (in press), with partial coverage photogrammetric 3D data acquired with an UAV (unmanned aerial vehicle). First, parametric bootstrap is a straightforward empirical method to account for error propagation in multiple modeling steps. Second, one of the modeling steps involves model parameter estimation with a large set of observations from spatially compact areas (i.e., the ALS patches). Here the model parameter covariances that are the basis in model-based estimation could be biasedly estimated as a result of the spatially auto-correlated observations. Simulations on a spatially consistent population could investigate this effect.

Table 7. Relative efficiencies of MA and HY estimators in simulated sampling (*paper III*). Values > 1 are bolded and indicate an increase in precision or accuracy relative to the direct estimation using field plots only. w/ PS – with post-stratification, w/o PS – without post-stratification.

Time	Stratum	MA			HY		
		$RE_{\widehat{SE}}$	RE_{SE}	RE_{RMSE}	$RE_{\widehat{SE}}$	RE_{SE}	RE_{RMSE}
	Nonforest	**1.62**	**1.54**	**1.42**	**1.30**	**1.68**	**1.37**
	Young	**1.49**	**1.58**	**1.54**	**1.46**	**2.10**	0.75
	Low	**1.31**	**1.69**	**1.55**	**1.10**	**1.87**	**1.70**
	Medium	**1.52**	**1.48**	**1.46**	**1.40**	**1.73**	**1.08**
	High	**1.63**	**1.50**	**1.47**	**1.49**	**1.82**	**1.46**
	All w/ PS	**1.41**	**1.53**	**1.45**	**1.30**	**1.83**	0.92
	All w/o PS	**1.56**	**1.71**	**1.72**	**1.24**	**1.89**	**1.11**
	Nonforest	**1.61**	**1.45**	**1.30**	**1.12**	**1.62**	**1.02**
	Young	**1.68**	**1.90**	**1.89**	**1.29**	**1.96**	**1.20**
	Low	**1.30**	**1.66**	**1.46**	**1.03**	**1.82**	**1.16**
	Medium	**1.65**	**1.62**	**1.60**	**1.65**	**1.77**	**1.18**
	High	**1.80**	**1.65**	**1.66**	**1.40**	**1.86**	**1.49**
	All w/ PS	**1.46**	**1.66**	**1.55**	**1.20**	**1.81**	**1.77**
	All w/o PS	**1.56**	**1.80**	**1.79**	**1.14**	**1.81**	**1.75**
	Nonforest	0.84	0.77	0.72	**1.49**	**2.13**	0.91
	Young	0.89	0.89	0.86	**2.25**	**2.79**	0.36
	Low	0.97	0.93	0.85	**1.42**	**1.31**	0.55
	Medium	**1.04**	**1.03**	0.99	**3.23**	**2.46**	0.57
	High	**1.32**	**1.30**	**1.26**	**4.78**	**3.65**	**1.36**
	All w/ PS	**1.04**	**1.02**	1.00	**2.56**	**2.60**	0.68
	All w/o PS	0.97	0.98	0.98	**2.83**	**3.48**	0.86

5. Conclusions and perspective

This thesis contributes with new simulative methodologies that facilitate the assessment of estimator properties following complex forest surveys that utilize auxiliary data. Experience has been gained with change estimation following repeated ALS sampling. This type of survey emerged in a context of recent efforts to devise cost effective solutions to increase local estimation precision of certain forest parameters in large-area surveys. The results reinforced previous findings, showing that ALS strip sampling supplementing the field survey substantially increase the estimation accuracy of AGB stocks. For change estimation however, this might not always be the case. Here the ALS survey did not improve change estimation. This matter requires further investigations. One direction would be to optimize the timeframe for the surveys, allowing the changes to become large enough for a more precise estimation, or to allow the change to be modeled directly. In the absence of a probabilistic field sample, as it may be the case of developing countries with poor infrastructure of the lack of an established NFI, the hybrid estimation remains as the sole alternative. In the context of HY estimation, the experience gained with ALS sampling paves the way for promising space LiDAR technology like ICESat-2 (Ice, Cloud, and land Elevation Satellite 2) or GEDI (Global Ecosystem Dynamics Investigation) to be used as a sampling tool for global carbon monitoring. This type of technology could enable more unified and transparent methodologies for carbon stocks monitoring across the countries.

Although post-stratification did not improve the change estimation precision, it retains its merit of enabling detailed reporting at more local scales. For instance, a unique post-stratified methodology could be used for countrywide change estimation, and in the same time provide change information at regional and sub-regional scale. Countrywide estimates would be used for international reporting, and regional estimates would enable national governments to adopt more efficient differentiated policies tailored to regional particularities. Moreover, the regional estimates would be consistent with the overall national estimates (i.e. the whole equals the sum of the parts). This approach fits well with programs like REDD (reducing emissions from deforestation and forest degradation) in the developing countries, allowing the governments to report credible carbon stock changes as well as to direct the financial incentives to local communities proportionally with the success of implementing REDD policies.

References

Andersen, H.-E., Barrett, T.M., Winterberger, K., Strunk, J., and Temesgen, H. 2009. Estimating forest biomass on the western lowlands of the Kenai Peninsula of Alaska using airborne LiDAR and field plot data in a model-assisted sampling design. *In* IUFRO Division 4 conference, extending forest inventory and monitoring over time and space, Quebec City, Canada.

Andersen, H.-E., Strunk, J., and Temesgen, H. 2011. Using Airborne Light Detection and Ranging as a Sampling Tool for Estimating Forest Biomass Resources in the Upper Tanana Valley of Interior Alaska. Western Journal of Applied Forestry **26**(4): 157-164.

Axelsson, P. 2000. DEM generation from laser scanner data using adaptive TIN models. International Archives of the Photogrammetry and Remote Sensing **33 (B4)**: 111–118.

Barnes, R.J. 1991. The variogram sill and the sample variance. Mathematical geology **23**(4): 673-678.

Barth, A., Lind, T., and Ståhl, G. 2012. Restricted imputation for improving spatial consistency in landscape level data for forest scenario analysis. Forest Ecology and Management **272**(0): 61-68.

Barth, A., Wallerman, J., and Stahl, G. 2009. Spatially consistent nearest neighbor imputation of forest stand data. Remote Sensing of Environment **113**(3): 546-553.

Bjørdal, I., and Bjørkelo, K. 2006. AR5 klassifikasjonssystem. Klassifikasjon av arealressurser. Skog og landskap.

Bollandsås, O.M., Gregoire, T.G., Næsset, E., and Øyen, B.-h. 2013. Detection of biomass change in a Norwegian mountain forest area using small footprint airborne laser scanner data. Statistical Methods & Applications **22**(1): 113-129.

Coops, N.C., Tompaski, P., Nijland, W., Rickbeil, G.J.M., Nielsen, S.E., Bater, C.W., and Stadt, J.J. 2016. A forest structure habitat index based on airborne laser scanning data. Ecological Indicators **67**: 346-357.

Ene, L.T., Næsset, E., and Gobakken, T. 2016a. Simulation-based assessment of sampling strategies for large-area biomass estimation using wall-to-wall and partial coverage airborne laser scanning surveys. Remote Sensing of Environment **176**: 328-340

Ene, L.T., Næsset, E., Gobakken, T., Bollandsås, O.M., Mauya, E.W., and Zahabu, E. 2017. Large-scale estimation of change in aboveground biomass in miombo woodlands using airborne laser scanning and national forest inventory data. Remote Sensing of Environment **188**: 106-117.

Ene, L.T., Næsset, E., Gobakken, T., Gregoire, T.G., Ståhl, G., and Nelson, R. 2012. Assessing the accuracy of regional LiDAR-based biomass estimation using a simulation approach. Remote Sensing of Environment **123**: 579-592.

Ene, L.T., Næsset, E., Gobakken, T., Mauya, E.W., Bollandsås, O.M., Gregoire, T.G., Ståhl, G., and Zahabu, E. 2016b. Large-scale estimation of aboveground biomass in miombo woodlands using airborne laser scanning and national forest inventory data. Remote Sensing of Environment **186**: 626-636.

Frey, C., Penman, J., Hanle, L., Monni, S., and Ogle, S. 2006. 2006 IPCC Guidelines for National Greenhouse Gas Inventories Institute for Global Environmental Strategies (IGES), Hayama Kanagawa, Japan.

Gagliasso, D., Hummel, S., and Temesgen, H. 2014. A Comparison of Selected Parametric and Non-Parametric Imputation Methods for Estimating Forest Biomass and Basal Area. Open Journal of Forestry **4**(1): 42-48.

Gobakken, T., Næsset, E., Nelson, R., Bollandsas, O.M., Gregoire, T.G., Stahl, G., Holm, S., Orka, H.O., and Astrup, R. 2012. Estimating biomass in Hedmark County, Norway using national forest inventory field plots and airborne laser scanning. Remote Sensing of Environment **123**: 443-456.

Grafström, A., and Ringvall, A.H. 2013. Improving forest field inventories by using remote sensing data in novel sampling designs. Canadian Journal of Forest Research **43**(11): 1015-1022.

Grafström, A., Saarela, S., and Ene, L.T. 2014. Efficient sampling strategies for forest inventories by spreading the sample in auxiliary space. Canadian Journal of Forest Research **44**(10): 1156-1164.

Gregoire, T.G. 1998. Design-based and model-based inference in survey sampling: appreciating the difference. Canadian Journal of Forest Research **28**(10): 1429-1447.

Gregoire, T.G., Næsset, E., McRoberts, R.E., Ståhl, G., Andersen, H.-E., Gobakken, T., Ene, L., and Nelson, R. 2016a. Statistical rigor in LiDAR-assisted estimation of aboveground forest biomass. Remote Sensing of Environment **173**: 98-108.

Gregoire, T.G., Ringvall, A.H., Ståhl, G., and Næsset, E. 2016b. Conditioning post-stratified inference following two-stage, equal-probability sampling. Environmental and Ecological Statistics **23**(1): 141-154.

Gregoire, T.G., Ståhl, G., Næsset, E., Gobakken, T., Nelson, R., and Holm, S. 2011. Model-assisted estimation of biomass in a LiDAR sample survey in Hedmark County, Norway. Canadian Journal of Forest Research **41**(1): 83-95.

Gustafson, E.J., Shifley, S.R., Mladenoff, D.J., Nimerfro, K.K., and He, H.S. 2000. Spatial simulation of forest succession and timber harvesting using LANDIS. Canadian Journal of Forest Research **30**(1): 32-43.

Horvitz, D.G., and Thompson, D.J. 1952. A Generalization of Sampling Without Replacement From a Finite Universe. Journal of the American Statistical Association **47**(260): 663-685.

IPCC. 2006. 2006 IPCC Guidelines for National Greenhouse Gas Inventories. Institute for Global Environmental Strategies (IGES), Hayama Kanagawa, Japan.

IPCC. 2014. Climate Change 2014: Synthesis Report. Contribution of Working Groups I, II and III to the Fifth Assessment Report of the Intergovernmental Panel on Climate Change. IPCC.

Kangas, A., Myllymäki, M., Gobakken, T., and Næsset, E. 2016. Model-assisted forest inventory with parametric, semiparametric, and nonparametric models. Canadian Journal of Forest Research **46**(6): 855-868.

Koch, B. 2010. Status and future of laser scanning, synthetic aperture radar and hyperspectral remote sensing data for forest biomass assessment. ISPRS Journal of Photogrammetry and Remote Sensing **65**(6): 581-590.

Lämås, T., and Eriksson, L.O. 2003. Analysis and planning systems for multiresource, sustainable forestry: The Heureka research programme at SLU. Canadian Journal of Forest Research **33**(3): 500-508.

Lone, K., van Beest, F.M., Mysterud, A., Gobakken, T., Milner, J.M., Ruud, H.-P., and Loe, L.E. 2014. Improving broad scale forage mapping and habitat selection analyses with airborne laser scanning: the case of moose. Ecosphere **5**(11): 1-22.

Maclean, G.A., and Krabill, W.B. 1986. Gross-Merchantable Timber Volume Estimation Using an Airborne Lidar System. Canadian Journal of Remote Sensing **12**(1): 7-18.

Magnussen, S., Köhl, M., and Olschofsky, K. 2014. Error propagation in stock-difference and gain–loss estimates of a forest biomass carbon balance. European Journal of Forest Research **133**(6): 1137-1155.

Magnussen, S., Næsset, E., and Gobakken, T. 2015. LiDAR-supported estimation of change in forest biomass with time-invariant regression models. Canadian Journal of Forest Research **45**(11): 1514-1523.

Maltamo, M., Bollandsås, O.M., Gobakken, T., and Næsset, E. 2016. Large-scale prediction of aboveground biomass in heterogeneous mountain forests by means of airborne laser scanning. Canadian Journal of Forest Research **46**(9): 1138-1144.

Marklund, L.G. 1988. Biomass functions for pine, spruce and birch in Sweden. Swedish University of Agricultural Sciences, Department of Forest Survey, Umeå.

McRoberts, R.E., Domke, G.M., Chen, Q., Næsset, E., and Gobakken, T. 2016. Using genetic algorithms to optimize k-Nearest Neighbors configurations for use with airborne laser scanning data. Remote Sensing of Environment **184**: 387-395.

McRoberts, R.E., Næsset, E., and Gobakken, T. 2015a. Optimizing the k-Nearest Neighbors technique for estimating forest aboveground biomass using airborne laser scanning data. Remote Sensing of Environment **163**: 13-22.

McRoberts, R.E., Næsset, E., Gobakken, T., and Bollandsås, O.M. 2015b. Indirect and direct estimation of forest biomass change using forest inventory and airborne laser scanning data. Remote Sensing of Environment **164**: 36-42.

Næsset, E. 1997. Estimating timber volume of forest stands using airborne laser scanner data. Remote Sensing of Environment **61**(2): 246 - 253.

Næsset, E. 2005. Towards a laser-scanner based biomass monitoring system. *In* SNS Meeting, Forest Inventory and Planning in Nordic Countries, Sjusjøen, Norway. pp. 117-119.

Næsset, E. 2014. Area-Based Inventory in Norway – From Innovation to an Operational Reality. *In* Forestry Applications of Airborne Laser Scanning: Concepts and Case Studies. *Edited by* M. Maltamo and E. Næsset and J. Vauhkonen. Springer Netherlands, Dordrecht. pp. 215-240.

Næsset, E., Bollandsås, O.M., Gobakken, T., Gregoire, T.G., and Ståhl, G. 2013a. Model-assisted estimation of change in forest biomass over an 11 year period in a sample survey supported by airborne LiDAR: A case study with post-stratification to provide "activity data". Remote Sensing of Environment **128**: 299-314.

Næsset, E., Gobakken, T., Bollandsås, O.M., Gregoire, T.G., Nelson, R., and Ståhl, G. 2013b. Comparison of precision of biomass estimates in regional field sample surveys and airborne LiDAR-assisted surveys in Hedmark County, Norway. Remote Sensing of Environment **130**(0): 108 - 120.

Næsset, E., Gobakken, T., Holmgren, J., Hyyppa, H., Hyyppa, J., Maltamo, M., and Nilsson, M. 2004. Laser Scanning of Forest Resources: The Nordic Experience. Scandinavian Journal of Forest Research **19**(6): 482.

Nelson, R. 2013. How did we get here? An early history of forestry lidar1. Canadian Journal of Remote Sensing **39**(sup1): S6-S17.

Nelson, R., Gobakken, T., Næsset, E., Gregoire, T.G., Ståhl, G., Holm, S., and Flewelling, J. 2012. Lidar sampling — Using an airborne profiler to estimate forest biomass in Hedmark County, Norway. Remote Sensing of Environment **123**: 563-578.

Nelson, R., Krabill, W., and Tonelli, J. 1988. Estimating forest biomass and volume using airborne laser data. Remote Sensing of Environment **24**(2): 247-267.

Økseter, R., Bollandsås, O.M., Gobakken, T., and Næsset, E. 2015. Modeling and predicting aboveground biomass change in young forest using multi-temporal airborne laser scanner data. Scandinavian Journal of Forest Research **30**(5): 458-469.

Packalén, P., Heinonen, T., Pukkala, T., Vauhkonen, J., and Maltamo, M. 2011. Dynamic Treatment Units in Eucalyptus Plantation. Forest Science **57**(5): 416-426.

Pan, Y., Birdsey, R.A., Fang, J., Houghton, R., Kauppi, P.E., Kurz, W.A., Phillips, O.L., Shvidenko, A., Lewis, S.L., Canadell, J.G., Ciais, P., Jackson, R.B., Pacala, S.W., McGuire, A.D., Piao, S., Rautiainen, A., Sitch, S., and Hayes, D. 2011. A Large and Persistent Carbon Sink in the World's Forests. Science **333**(6045): 988-993.

Puliti, S., Saarela, S., Gobakken, T., Ståhl, G., and Naesset, E. 2017 (in press). Combining UAV and Sentinel-2 auxiliary data for forest growing stock volume estimation through hierarchical model-based inference. Remote Sensing of Environment.

Ribeiro, P.J., and Diggle, P.J. 2016. geoR: Analysis of Geostatistical Data.

Ringvall, A.H., Ståhl, G., Ene, L.T., Næsset, E., Gobakken, T., and Gregoire, T.G. 2016. A poststratified ratio estimator for model-assisted biomass estimation in sample-based airborne laser scanning surveys. Canadian Journal of Forest Research **46**(11): 1386-1395. doi: 10.1139/cjfr-2016-0158.

Royall, R.M. 1970. On Finite Population Sampling Theory Under Certain Linear Regression Models. Biometrika **57**(2): 377-387.

Saarela, S., Andersen, H.-E., Grafström, A., Schnell, S., Gobakken, T., Næsset, E., Nelson, R.F., McRoberts, R.E., Gregoire, T.G., and Ståhl, G. 2017. A new prediction-based variance estimator for two-stage model-assisted surveys of forest resources. Remote Sensing of Environment **192**: 1-11.

Saarela, S., Holm, S., Grafström, A., Schnell, S., Næsset, E., Gregoire, T.G., Nelson, R.F., and Ståhl, G. 2016. Hierarchical model-based inference for forest inventory utilizing three sources of information. Annals of Forest Science **73**(4): 895-910.

Saarela, S., Schnell, S., Grafström, A., Tuominen, S., Nordkvist, K., Hyyppä, J., Kangas, A., and Ståhl, G. 2015. Effects of sample size and model form on the accuracy of model-based estimators of growing stock volume. Canadian Journal of Forest Research **45**(11): 1524-1534.

Särndal, C.-E., Swensson, B., and Wretman, J.H.k. 1992. Model Assisted Survey Sampling. Springer-Verlang, New York.

Skowronski, N.S., Clark, K.L., Gallagher, M., Birdsey, R.A., and Hom, J.L. 2014. Airborne laser scanner-assisted estimation of aboveground biomass change in a temperate oak–pine forest. Remote Sensing of Environment **151**: 166-174.

Ståhl, G., Holm, S., Gregoire, T.G., Gobakken, T., Næsset, E., and Nelson, R. 2011. Model-based inference for biomass estimation in a LiDAR sample survey in Hedmark County, Norway. Canadian Journal of Forest Research **41**(1): 96-107.

Ståhl, G., Saarela, S., Schnell, S., Holm, S., Breidenbach, J., Healey, S.P., Patterson, P.L., Magnussen, S., Næsset, E., McRoberts, R.E., and Gregoire, T.G. 2016. Use of models in large-area forest surveys: comparing model-assisted, model-based and hybrid estimation. Forest Ecosystems **3**(1): 5.

Strîmbu, V.F., Ene, L.T., Gobakken, T., Gregoire, T.G., Astrup, R., and Næsset, E. 2017. Post-stratified change estimation for large-area forest biomass using repeated ALS strip sampling. Canadian Journal of Forest Research **47**(6): 839-847.

Tokola, T., and Shrestha, S.M. 1999. Comparison of cluster-sampling techniques for forest inventory in southern Nepal. Forest Ecology and Management **116**(1–3): 219-231.

Tomter, S.M., Hylen, G., and Nilsen, J.-E. 2010. Development of Norway's National Forest Inventory. . *In* National Forest Inventories - Pathways for Common Reporting. Springer. pp. 411-424.

Tomppo, E., Malimbwi, R., Katila, M., Mäkisara, K., Henttonen, H.M., Chamuya, N., Zahabu, E., and Otieno, J. 2014. A sampling design for a large area forest inventory: case Tanzania. Canadian Journal of Forest Research **44**(8): 931-948.

Tomppo, E., Olsson, H., Ståhl, G., Nilsson, M., Hagner, O., and Katila, M. 2008. Combining national forest inventory field plots and remote sensing data for forest databases. Remote Sensing of Environment **112**(5): 1982-1999.

Wulder, M.A., White, J.C., Nelson, R.F., Næsset, E., Ørka, H.O., Coops, N.C., Hilker, T., Bater, C.W., and Gobakken, T. 2012. Lidar sampling for large-area forest characterization: A review. Remote Sensing of Environment **121**: 196-209.

Zolkos, S.G., Goetz, S.J., and Dubayah, R. 2013. A meta-analysis of terrestrial aboveground biomass estimation using lidar remote sensing. Remote Sensing of Environment **128**: 289-298.

Paper I Strîmbu, V.F., Ene, L.T. & Næsset, E. 2016. Spatially consistent imputations of forest data under a semivariogram model. - Canadian Journal of Forest Research 46: 1145-1156. DOI: 10.1139/cjfr-2016-0068
Paper II Strîmbu, V.F., Ene, L.T., Gobakken, T., Gregoire, T.G., Astrup, R. & Næsset, E. 2017. Post-stratified change estimation for large-area forest biomass using repeated ALS strip sampling. - Canadian Journal of Forest Research 47: 839-847. DOI: 10.1139/cjfr-2017-0031
Paper III Strîmbu, V.F., Ene, L.T., Gobakken, T. & Næsset, E. Simulative assessment of model assisted and hybrid estimation of change using repeated ALS sampling (Manuscript)

ISBN: 978-82-575-1465-5
ISSN: 1894-6402

Norwegian University
of Life Sciences

Postboks 5003
NO-1432 Ås, Norway
+47 67 23 00 00
www.nmbu.no